ACS ES&T Engineering

Open Access

pubs.acs.org/estengg

Article

Thermal Phase Transition and Rapid Degradation of Forever Chemicals (PFAS) in Spent Media Using Induction Heating

Feng Xiao,* Pavankumar Challa Sasi, Ali Alinezhad, Runze Sun, and Mansurat Abdulmalik Ali

Cite This: *ACS EST Engg.* 2023, 3, 1370−1380

Read Online

ACCESS | Metrics & More | Article Recommendations | Supporting Information

ABSTRACT: In this study, we have developed an innovative thermal degradation strategy for treating per- and polyfluoroalkyl substance (PFAS)-containing solid materials. Our strategy satisfies three criteria: the ability to achieve near-complete degradation of PFASs within a short timescale, nonselectivity, and low energy cost. In our method, a metallic reactor containing a PFAS-laden sample was subjected to electromagnetic induction that prompted a rapid temperature rise of the reactor via the Joule heating effect. We demonstrated that subjecting PFASs (0.001−12 μmol) to induction heating for a brief duration (e.g., <40 s) resulted in substantial degradation (>90%) of these compounds, including recalcitrant short-chain PFASs and perfluoroalkyl sulfonic acids. This finding prompted us to conduct a detailed study of the thermal phase transitions of PFASs using thermogravimetric analysis and differential scanning calorimetry (DSC). We identified at least two endothermic DSC peaks for anionic, cationic, and zwitterionic PFASs, signifying the melting and evaporation of the melted PFASs. Melting and evaporation points of many PFASs were reported for the first time. Our data suggest that the rate-limiting step in PFAS thermal degradation is linked with phase transitions (e.g., evaporation) occurring on different time scales. When PFASs are rapidly heated to temperatures similar to those produced during induction heating, the evaporation of melted PFAS slows down, allowing for the degradation of the melted PFAS.

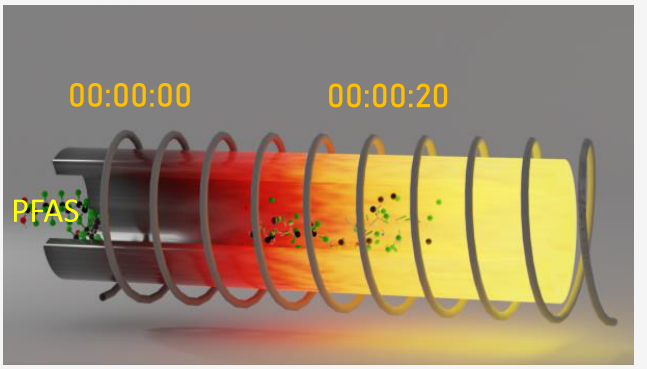

KEYWORDS: *joule effect, GAC, resin, melting point, evaporation point*

INTRODUCTION

Per- and polyfluoroalkyl substances (PFASs) are synthetic chemicals produced for various industrial and commercial products such as cosmetics,[1] facemasks,[2] food containers,[3,4] nonstick cookware,[5] baking papers,[6] and aqueous film-forming foams (AFFFs).[7,8] Due to their widespread use, PFASs have been found in various environmental compartments, raising concerns about their potential health risks.[9−13] Of particular concern is the presence of PFAS in drinking water supplies.[14,15] On March 14, 2023, the U.S. Environmental Protection Agency (EPA) released the proposed PFAS National Primary Drinking Water Regulation, which aims to establish maximum contaminant levels or a hazard index for six primary PFAS, perfluorooctanoic acid (PFOA), perfluorooctanesulfonic acid (PFOS), perfluorononanoic acid (PFNA), hexafluoropropylene oxide dimer acid (HFPO-DA, commonly known as GenX Chemicals), perfluorohexane sulfonic acid (PFHxS), and perfluorobutane sulfonic acid (PFBS). If finalized, the regulation would require U.S. public water systems to monitor and reduce PFAS contamination in drinking water. Similar regulations are being developed or implemented in many other countries and regions, including the European Union,[16] Canada,[17,18] and China,[19] making the protection of drinking water sources from PFAS contamination a global priority.

The use of granular activated carbon (GAC) and anion exchange (AIX) resins for the sorptive removal of PFASs from water has become a common practice in practical applications.[20−24] Single-use and nonionic resins have been recently explored as a potential alternative to GAC and regenerable AIX resins for removing short-chain PFASs from water.[25,26] The disposal of exhausted GAC and resins can present challenges, as the spent media contain PFAS. Regenerating PFAS-laden spent GAC and resins using inorganic salts (e.g., NaCl) or methanol alone is difficult,[27−29] because PFAS molecules are far more hydrophobic than inorganic anions such as Cl^-. Thus, there is an urgent need for effective technologies to minimize, attenuate, and remediate PFASs in spent media. An ideal treatment method for solid wastes containing PFAS would be

Received: March 19, 2023
Revised: April 13, 2023
Accepted: April 17, 2023
Published: April 26, 2023

https://doi.org/10.1021/acsestengg.3c00114
ACS EST Engg. 2023, 3, 1370−1380

effective for a broad spectrum of PFAS, achieve rapid degradation, and be suitable for use in rural or remote communities that lack centralized waste treatment facilities.

Thermal-based approaches have emerged as an attractive means[29−36] to decontaminate PFAS-laden GAC,[29,33,37−39] resins,[40] and other solid materials (e.g., soil,[30,38] biosolids,[41] and biomass[42]). Our group investigated conventional thermal treatment using regular ovens/furnaces as a means of degrading PFASs in soil[30] and spent GAC.[29,31,33] We now have a moderate level of understanding regarding the fate of PFAS during conventional heating: (1) thermal decomposition of PFAS proceeds through multistep free-radical reactions, including initiation, chain propagation, and termination;[33,36] (2) the addition of GAC or a resin (Amberlite XAD-2) can substantially accelerate the thermal decomposition of perfluorocarboxylic acids (PFCAs) and HFPO-DA at low and moderate temperatures (<400 °C);[33] (3) perfluoroalkyl sulfonic acids (PFSAs) require a relatively high temperature (≥450 °C) to decompose;[29,33] (4) polyfluoroalkyl substances are subject to thermal side-chain stripping on the nonfluorinated moiety[31] and more prone to degradation than perfluoroalkyl counterparts;[31] (5) the thermal degradation of PFAS yields various transient intermediates, including perfluoroalkenes, at low and moderate temperatures;[30−33] and (6) substantial mineralization (>90%) of PFOA and potassium salt of PFOS (K-PFOS) occurs at 700 °C and above.[29]

Despite the insights gained from recent studies,[29−31,33−35,40,43] much is still unknown about the phase transitions (such as melting and evaporation) of these compounds,[36] which is crucial for developing effective thermal remediation plans and understanding their behavior in other thermal processes such as cooking, baking, and firefighting in which PFAS-containing products are used. Furthermore, the rate-limiting steps or factors controlling PFAS thermal decomposition kinetics also remain elusive, and little[33] or no effort has been devoted so far for accelerating PFAS thermal decomposition. Traditional methods such as smoldering[38] and thermal desorption[44] are energy-intensive and time-consuming, while incineration is prohibitively expensive and can lead to the formation of toxic chlorinated/brominated dioxins and furans.[45−48] The U.S. DoD has placed a temporary halt on the burning or incineration of PFAS as a destruction and disposal method.[49] Pyrolysis has also shown to be effective in degrading PFAS,[30,32] but is also costly. Thus, there is a pressing need for alternative, cost-effective thermal methods for PFAS degradation in solid materials, such as the spent media.

The purpose of the present study was twofold: (a) to develop an innovative and practical technique through which ultrafast degradation of short- and long-chain PFAS on spent media can be achieved; and (b) to better understand thermal phase transitions (e.g., melting and evaporation) of PFASs at a fundamental level. We first present an innovative PFAS thermal treatment technology through which the degradation of PFAS can be achieved in a matter of a few minutes. The method is based on the Joule heating effect, where heat is generated in a metallic reactor by electromagnetic induction without direct contact between the induction heater and the reactor. Additional heat is produced by hysteresis losses for magnetic materials during thermal treatment.[50] Compared to conventional thermal techniques (e.g., flame heating, furnaces, and ovens), induction heating offers a fast heating rate and is potentially inexpensive.

We then conducted a series of fundamental studies to investigate the thermochemical properties of PFAS and explored several mechanisms that could explain the observed ultrafast degradation of PFAS during induction heating. Published studies with these objectives in mind are very few[33,43] and were seldom carried out in a systematic manner. Consistent with existing literature,[29,33] we tested the hypothesis that phase transitions such as evaporation could be the rate-limiting step. Because the costs of thermal treatment rise significantly with the residence time, identification of the rate-limiting steps could lead to technological improvements and remediation cost reduction.

MATERIALS AND METHODS

Induction Heating Device, PFASs, and Solid Samples. We included all six PFASs in the EPA's proposed PFAS National Primary Drinking Water Regulation as well as five PFCAs that are frequently observed in the natural environment (Table S1), including perfluorobutyric acid (PFBA, C4), perfluoropentanoic acid (PFPeA, C5), perfluoroheptanoic acid (PFHpA, C7), perfluorodecanoic acid (PFDA, C10), and perfluoroundecanoic acid (PFUnDA, C11). In addition to these 11 perfluorinated chemicals, this study also included three cationic and zwitterionic PFASs (Table S1), perfluorooctaneamido betaine (PFOAB), perfluorooctaneamido ammonium salt (PFOAAmS), and *N*-(3-perfluoroalkylsulfonamidopropan-1-yl)-N,N,Ntrimethylammonium (C8-*N*-TAmP-FASA[7]) that is also named as perfluorooctanesulfonamido ammonium salt (PFOSAmS) in other studies.[31,51] The GAC was Filtrasorb 200 (Calgon Carbon Corporation, PA) (BET surface area, 691.4 m^2/g; microporosity, 0.3 cm^3/g; mesoporosity, 0.07 cm^3/g; Figure S2). The resin was a single-use AIX resin (AmberChrom® 1X8, formerly Dowex ® 1X8).

The induction heating device was a handheld induction-heating tool (Bolt Buster) procured from LACE Technologies, Inc (Addison, IL, USA). Stainless-steel reactors (7 mL; 45 mm in height and 19 mm in outside diameter) with a stainless-steel screw lid were obtained from the QAQC Lab Inc. (White Stone, VA, USA) for induction heating experiments. The reactor temperature during induction heating was recorded using a Digi-Sense dual-laser infrared thermometer (Cole Parmer, IL, USA) in a continuous scan mode connected to a computer with an infrared thermometer software package (Figure S1).

Induction Heating Experiment #1: PFASs with or without the Presence of GAC. A known volume (0.2 mL) of stock solutions (0.1 mmol/L in methanol, Optima LC/MS grade) of PFCAs, K-PFSAs, and HFPO-DA was added into a stainless-steel reactor (without a lid) and dried overnight in a forced-air oven (Cascade Tek, Cornelius, OR, USA) at 25 °C. After that, the reactor was screwed tightly closed using clamps and inductively heated (Figure S1) for a maximum operating time of 2 min. The induction heating of PFASs was conducted in an air atmosphere. After heating, it took approximately 65 s for the reactor to cool down to room temperature.

After induction heating and cooldown, a known volume of methanol and ammonium acetate at 100 mol/L was added.[29] The residual PFASs and degradation products were analyzed using an ultrahigh-pressure liquid chromatograph connected to a high-resolution, time-of-flight mass spectrometer (Synapt G2-S, Waters Corporation, Milford, MA) (see SI). Degradation in this paper refers to the breakdown of PFASs into smaller molecules due to exposure to high temperatures. The

https://doi.org/10.1021/acsestengg.3c00114
ACS EST Engg. 2023, 3, 1370−1380

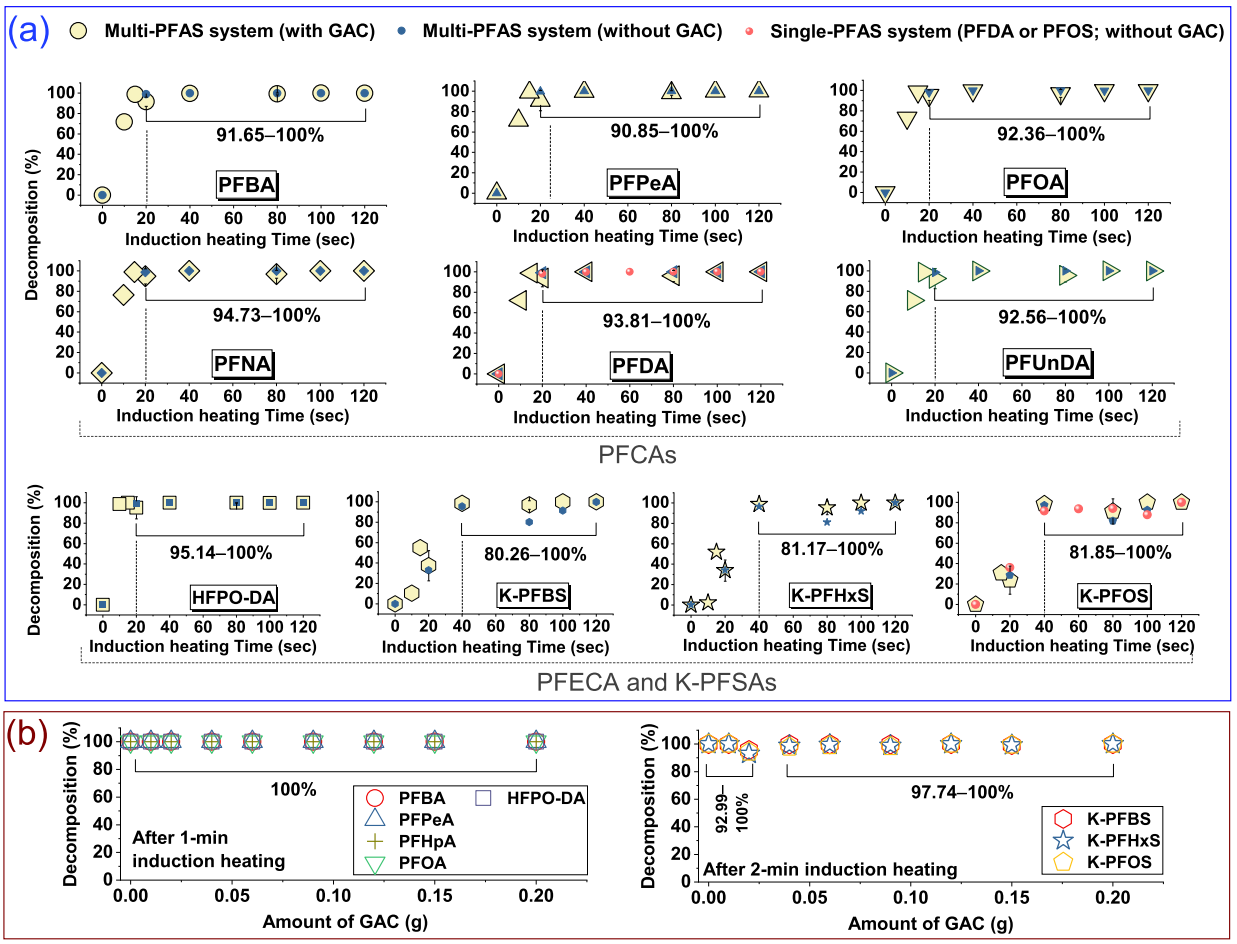

Figure 1. Induction heating (up to 2 min) of PFCAs, HFPO-DA, and K-PFSAs in an air atmosphere in a sealed steel reactor. (a): Initial mass of each PFAS was 0.02 μmol in multi-PFAS systems with or without GAC (0.1 g). To estimate the maximum degradation efficiency, the initial mass of PFDA and K-PFOS was increased to 12 μmol in certain single-PFAS treatment experiments. (b): Induction heating of PFAS preadsorbed on different amounts of GAC (0.01, 0.02, 0.04, 0.06, 0.09, 0.12, 0.15, and 0.2 g); the loadings (μmol/g_{GAC}) are as follows: HFPO-DA, 0.30−0.93; PFBA, 0.48−1.36; PFPeA, 0.50−0.79; PFHpA, 0.47−0.98; PFOA, 0.63−1.70, K-PFBS, 0.67−1.26; K-PFHxS, 0.56−1.45; and K-PFOS, 1.06−4.94. Decomposition efficiency was assigned to 100% if no measurable PFAS was found after the thermal treatment. Note that the actual PFAS heating time is longer than the induction heating time (e.g., 20 s) as it took approximately 65 s to cool down from ~845 °C to room temperature.

thermal degradation efficiency was calculated by comparing the residual mass of PFASs in the heated sample with that in nonheated controls.[29] In select experiments, distilled water instead of methanol was added to the reactor to measure water-extractable fluoride ions (F^-) by an F ion selective electrode (METTLER TOLEDO) on a Mettler Toledo pH/mV Meter (FiveEasy F20).

To examine the effect of GAC, the induction heating experiments described above were repeated by directly mixing a PFASs with GAC particles (0.1 g) to represent the PFAS molecules loosely associated with GAC particles.

Induction Heating Experiment #2: PFASs Preadsorbed on GAC and AIX Resin. In this experiment, PFBA, PFBS, PFPeA, PFHpA, PFHxS, PFOA, PFOS, and HFPO-DA were preadsorbed to GAC and resin in landfill leachate that was provided by Waste Management Inc. Because no measurable PFASs (n = 14; Table S1) were detected in microfiltered landfill leachate samples, these chemicals were spiked to landfill leachate in the laboratory to facilitate detection. Adsorption was performed in 50-mL sterile polypropylene vials[52] at initial concentrations of 1.92−45.5 μmol/L PFASs and 0.01−0.2 g GAC and 0.07 g AIX resin. The vials were shaken end-over-end at 22 °C for two days. After sorption, the supernatant fluid was decanted. The remaining PFAS-laden particles were freeze−dried and stored in a desiccator to reach room temperature. These PFAS-containing particles were split into two portions in a procedure described previously:[29] one portion of the particles was extracted using methanol amended with 100 mol/L ammonium acetate to determine PFASs on particles before heating.[29] The other portion of the PFAS-laden particles was placed in a precleaned, stainless-steel reactor. The reactor was sealed with a stainless-steel screw cap and heated by the induction-heating device (Figure S1) for a maximum operating time of 2 min. If a heating time exceeding 2 minutes was needed, the induction-heating tool was allowed to cool down for 3 min before being reused for heating the reactor.

Determination of Thermal Phase Transition Parameters of PFASs. We carried out a series of thermogravimetric analysis (TGA), differential thermogravimetry (DTG), and differential scanning calorimetry (DSC) experiments at the default heating rate (10 °C/min) in different atmospheres (O_2, CO_2, and N_2) (TGA/STD Q600; TA Instrument, DE). The first derivative of the DSC curve was used to determine inflection points or exothermic or endothermic peaks for in-depth interpretations. An endothermic peak on DSC curves is

https://doi.org/10.1021/acsestengg.3c00114
ACS EST Engg. 2023, 3, 1370−1380

a melting point (MP) if the sample weight does not undergo a significant change over the course of this peak or a sublimation peak if the sample weight decreases substantially below its MP.[53,54] To examine the effect of heating rate, we performed additional TGA analyses at different heating rates (5, 10, and 20 °C/min) using a TGA 8000TM instrument (Perkin Elmer).

The Arrhenius activation energies ($E_{A,evaporation}$) corresponding to the evaporation of melted PFOA and PFOS molecules were determined from the TGA data at appropriate temperature ranges (see below). PFAS mass loss due to evaporation can be described as:[55]

$$d\alpha/dt = k \times f(\alpha) \quad (1)$$

where $d\alpha/dt$ is the rate of evaporation, α is the fractional evaporation at any time, and k is the rate constant. The term $f(\alpha)$ is a function form of α. The rate constant is dependent upon the thermal treatment temperature (T) according to the Arrhenius equation:

$$k = A \times \exp(-E_{A,evaporation}/RT) \quad (2)$$

Plots of ln k versus $1/T$ would give the apparent activation energy.

Thermal Degradation of Gas-Phase PFOA and PFOS. As shown below, the evaporation of melted PFOA and K-PFOS molecules occurs at 46−155 and 277−450 °C, respectively. We previously performed thermal degradation experiments in a sealed reactor at temperatures where the degradation of gas-phase of PFOA (≥ 200 °C) and K-PFOS (≥400 °C) occurred.[30,33] The previous results[30,33] were used to estimate the Arrhenius activation energies ($E_{A,gas\text{-}phase\ degradation}$) corresponding to the gas-phase degradation of PFOA and PFOS in a pressured reactor.

Furthermore, we also carried out additional experiments of heating PFOA at ≥200 °C in a tube furnace under the flow of N_2, which is a nonpressured system (see SI for more details). The results were used to estimate $E_{A,gas\text{-}phase\ degradation}$ of PFOA in a nonpressured reactor.

RESULTS AND DISCUSSION

Induction Heating as an Innovative Thermal Approach for PFAS Degradation in Spent Media. Thermal treatment is a vital approach for the decontamination of spent or exhausted GAC laden with PFASs.[29,33,37,38,56] It is a common industry practice to regenerate the spent GAC at <300 °C or reactivate the spent carbon at 700−900 °C in N_2 for approximately 30 min. The thermal disposal of spent resins containing PFASs has only recently received attention.[40] In this study, we present induction heating as a promising means to achieve fast degradation of PFASs in the spent media. Induction heating is the process of heating electrically conductive materials such as metallic objects by rapidly fluctuating a magnetic field from positive to negative. Because the heat is generated inside a metallic object rather than by an external heat source, the object can be heated up very rapidly. Upon induction heating, the temperature of the steel reactor quickly increased from room temperature (22 °C) to ∼500 °C in 30 s, with a heating rate of 16 °C/s. Then, within another 30 s, the temperature rose to ∼845 °C (Table S2). The infrared thermometer underestimated the steel temperature by a large margin (Table S2). Infrared thermometers measure an object's temperature by collecting the infrared radiation emitted by the object, which can lead to inaccuracies when measuring low-emissivity materials like stainless steel.

As shown in Figures 1a and 2, substantial degradation (71−98%) of HFPO-DA and PFCAs was observed following an induction heating time of 10 s. A longer induction heating time of 40 s resulted in an even greater decomposition (>99.5%) (Figures 1a and 2). K-PFSAs were more thermally stable than PFCAs; a brief induction heating treatment for 20 s resulted in 28−34% degradation of all K-PFSAs, while a treatment time of 40 s increased the extent of degradation to >90%. Near-complete degradation of K-PFOS on the spent media was observed after the induction heating of 2−3 min (Figures 1a and 2). It took a slightly longer time to degrade K-PFSAs on the resin than on GAC (Figure 2). This may be related to the different thermal conductivities between GAC and the resin; however, the exact reason is unclear at this stage.

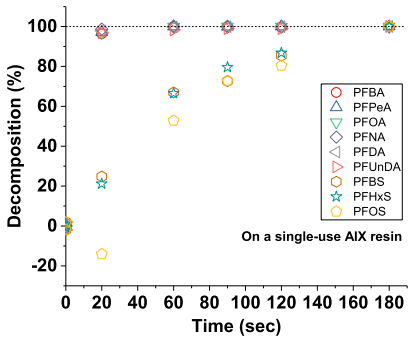

Figure 2. Induction heating of a mixture of PFASs preadsorbed on a single-use AIX resin in an air atmosphere. Loadings (μmol/g_{AIX}) are as follows: PFBA, 6.42−7.65; PFPeA, 1.65−2.05; PFOA, 2.58−3.30, PFNA, 13.2−17.8; PFDA, 8.86−10.9; PFUnDA, 10.3−12.5; K-PFBS, 2.56−3.15; K-PFHxS, 1.42−2.02; and K-PFOS, 2.42−3.15. Decomposition efficiency was assigned to 100% if no measurable PFASs were found after the thermal treatment. Note that the actual PFAS heating time is longer than the induction heating time (e.g., 20 s) as it took approximately 65 s to cool down from ∼845 °C to room temperature.

In selected experiments, we increased the initial mass of K-PFOS and PFDA to 12 μmol to facilitate the detection of degradation intermediates. Despite this high initial mass, induction heating resulted in greater than 5-log (99.999%) degradation of K-PFOS and PFDA within just 2 minutes (Figure 1b). Our previous study showed that the effect of the initial mass of PFASs on their thermal degradation is insignificant, provided appropriate temperatures (≥500 °C) and time (≥30 min) combinations are used.[29,30,33] No detectable transformation products[31,33] were observed in ultra-high performance liquid chromatography (UPLC)−quadrupole time-of-flight mass spectrometry (QToF)-mass spectrometry (MS)/MS analyses, indicating the rapid degradation of both parent PFAS compounds and transient intermediates during induction heating. Although this study did not measure the gaseous products of PFASs, our previous research demonstrated the rapid degradation of gaseous fluorinated compounds produced from PFASs, AFFFs, and surfactant concentrates.[32] The heating rate used in that study[32] was 400 °C/min, or 6.7 °C/s, which is comparable to the present work. We discovered that the type and intensity of gaseous products detected by gas chromatography−MS (GC−MS) sharply decreased with increasing temperature up to 890 °C.[32] Perfluoroheptene (C_7F_{14}) is a main gaseous thermal

https://doi.org/10.1021/acsestengg.3c00114
ACS EST Engg. 2023, 3, 1370−1380

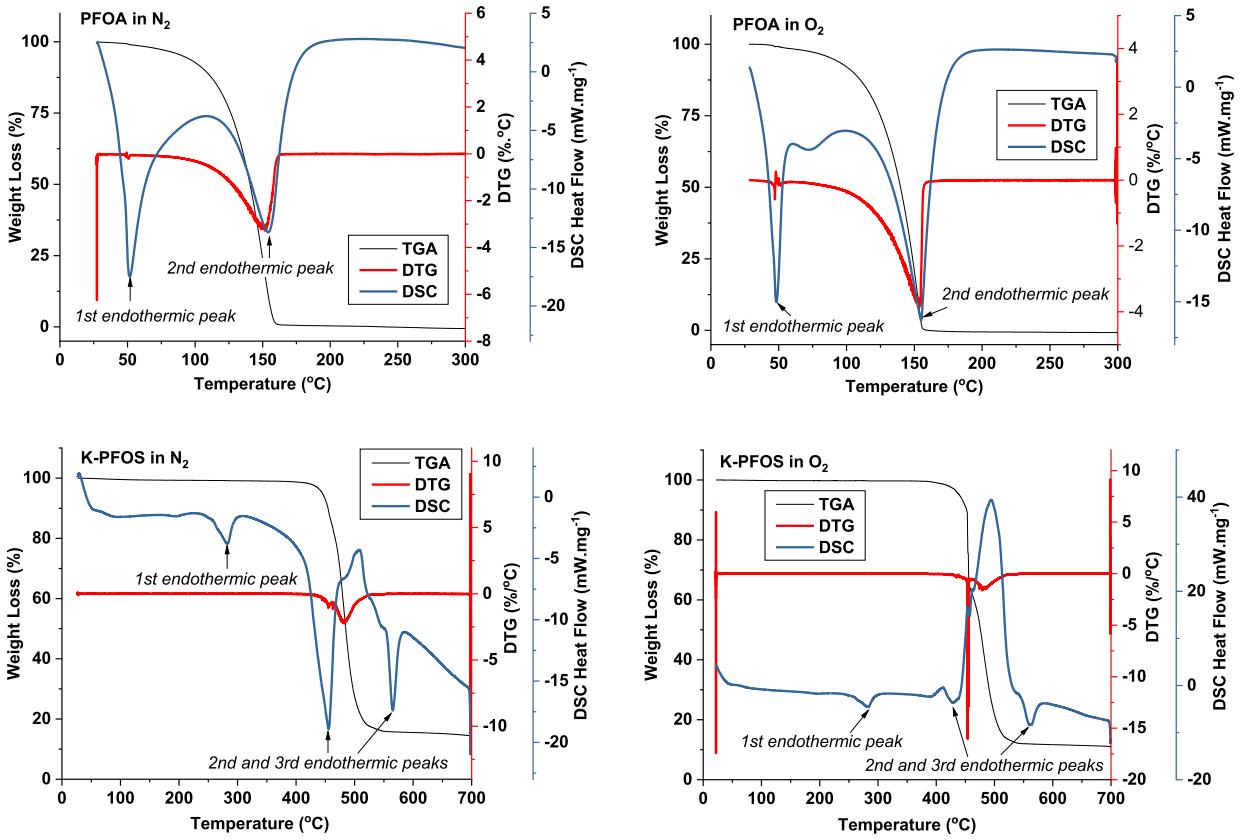

Figure 3. TGA, DTG, and DSC curves of PFOA and K-PFOS under N_2 and O_2. See Figures S3–S24 for results on all PFASs.

decomposition product of PFOA, PFOS, and cationic/zwitterionic precursor compounds.[32] We also showed that perfluoro-1-heptene (CAS: 355-63-5; BP: 81 °C) began to decompose at temperatures as low as 200 °C and underwent almost complete degradation upon heating at 890 °C for just 2 min.[32] Very few organofluorine compounds were detected when PFOA, PFOS, AFFFs, and surfactant concentrates were heated at 890 °C for 2 min.[32] These UPLC–QToF-MS/MS and GC–MS results are consistent with our results on the significant mineralization rate (up to 92 mol %) of PFOA and K-PFOS heated at 700 °C and above.[29] This temperature range falls within the range of induction heating employed in this study.

Furthermore, it is worth noting that GAC has a much higher thermal conductivity (0.4–1.36 W/(m K)[57,58]) than air (<0.051 W/(m K) at ≤400 °C[59]) at low temperatures, which enhances the thermal degradation of PFCA by adsorbing gas-phase PFCA molecules.[33] However, the impact of GAC becomes insignificant at temperatures of 400 °C and above, as the thermal conductivity of air increases considerably with temperature.[33] In this study, we observed no significant effect of GAC on the degradation of PFCAs and K-PFSAs (Figure 1a) during induction heating, as the reactor's temperature could reach up to 845 °C.

Mechanistic Considerations. On the basis of our previous findings,[29−31,33,36] we believe that the thermal degradation of PFASs involves the following stages when heated in an oven or furnace at a conventional rate (e.g., 10 °C/min), (I) melting (eq 3), (II) evaporation of melted molecules (eq 4), and (III) degradation of gas-phase PFAS molecules (eq 5):

$$\text{PFAS} \xrightarrow{\text{melting}} \text{PFAS (liquid)} \tag{3}$$

$$\text{PFAS (liquid)} \xrightarrow{\text{evaporation}} \text{PFAS (gaseous)} \tag{4}$$

$$\text{PFAS (gaseous)} \xrightarrow{\text{initiation}} \text{perfluoroalkyl radicals} \xrightarrow{\text{propagation}} \text{transient intermediates} \xrightarrow{\text{termination}} \text{final products} \tag{5}$$

In addition to the high efficiency of induction heating, the fast degradation of PFASs during induction heating may be attributed to the reduction of time spent on evaporation and thermal degradation of PFASs in the melting stage (eqs 6 and 7):

$$\text{PFAS} \xrightarrow{\text{melting}} \text{PFAS (liquid) and PFAS} \xrightarrow{\text{sublimation}} \text{PFAS (gas)} \tag{6}$$

$$\text{PFAS (liquid/gas)} \xrightarrow{\text{degradation}} \text{final products} \tag{7}$$

To better understand the role of phase transitions (melting and evaporation) of PFASs in their thermal degradation processes, which have not been well understood, we conducted (1) TGA-related analyses of PFASs and (2) compared the Arrhenius activation energies required for thermal phase transition and thermal degradation processes.

Thermal Phase Transitions of PFASs. TGA has previously proved to be useful in studying PFAS thermal behaviors in different atmospheres.[29,40] In this study, we utilized two related techniques, DTG and DSC, to study the

https://doi.org/10.1021/acsestengg.3c00114
ACS EST Engg. 2023, 3, 1370−1380

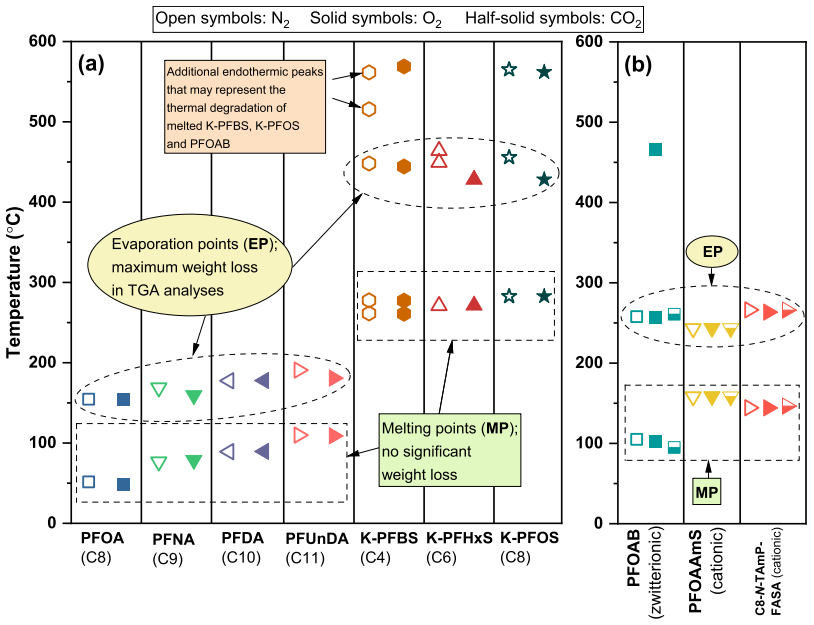

Figure 4. MP and EP of PFASs identified on DSC curves. Y-axis shows temperatures corresponding to endothermic peaks on DSC curves of (a) PFCAs and K-PFSAs and (b) cationic/zwitterionic polyfluoroalkyl substances. Figures S3−S24 display TGA and DSC curves for individual PFASs in different atmospheres.

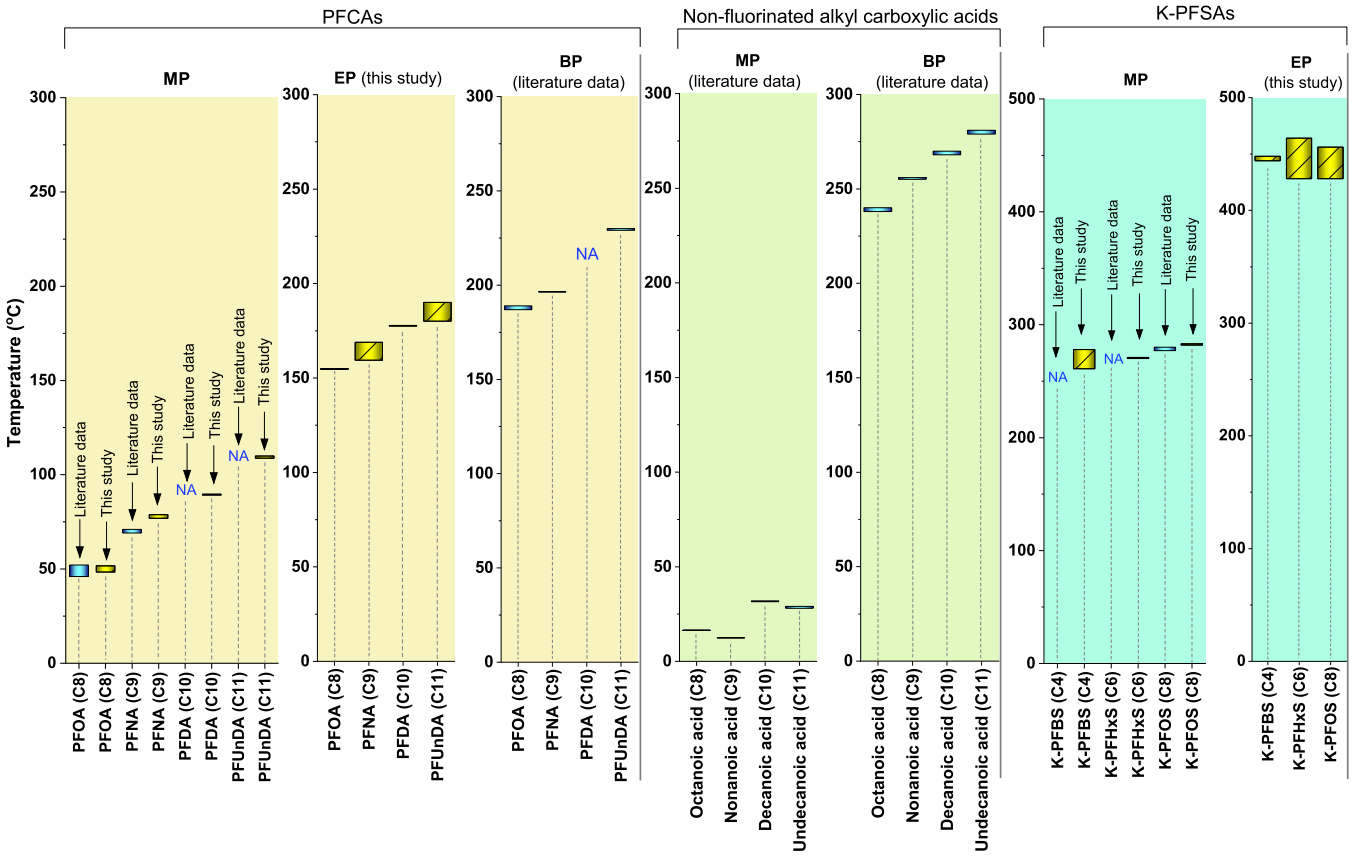

Figure 5. Floating columns showing the MP, EP, and BP temperature range for PFCAs, nonfluorinated alkyl carboxylic acids, and K-PFSAs. EPs for PFASs and nonfluorinated alkyl carboxylic acids are not available in the literature. NA: not available in the literature. Literature data were obtained from PubChem and SciFinder®. MPs and EPs of PFCAs and K-PFSAs were measured in N_2 and O_2 in this study (see Figure 4).

phase transitions of PFASs. These techniques provided valuable weight loss and heat flow information during the process (SI). At the default heating rate (10 °C), several major endothermic peaks were identified on DSC curves for every PFAS (Figures 5 and S3−S24). The first endothermic peak appeared at a relatively low temperature with no significant weight loss in PFASs (see TGA and DTG curves in Figures S3−S24 for all PFASs). We assigned this peak as the MP of

https://doi.org/10.1021/acsestengg.3c00114
ACS EST Engg. 2023, 3, 1370−1380

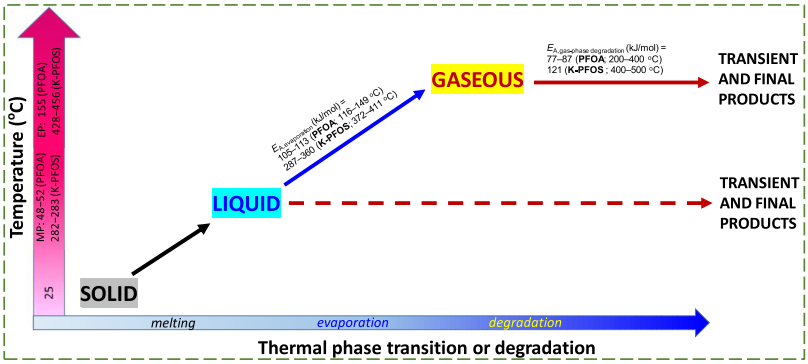

Figure 6. Illustration of the thermal phase transition and degradation of PFOA and K-PFOS.

PFASs (Figure 4). The close agreement in PFAS phase transition parameters (e.g., MP) in different atmospheres, as shown in Figure 4, provides a high level of confidence in the results. The DSC-derived MPs of PFOA (48−52 °C) and K-PFOS (283 °C) agree well with the literature values (46−52 °C for PFOA[53,60,61] and 277−280 °C for K-PFOS[62]).

A second endothermic peak was identified on the DSC curves at a higher temperature (e.g., 155 °C for PFOA) at which the weight loss rate reached the maximum according to TGA results (Figure 3). Our team had previously confirmed that PFOA thermal decomposition occurred very slowly at 150 °C in a sealed reactor,[33] indicating that the marked weight loss of PFOA at 155 °C (Figure 3) was primarily due to the evaporation of melted or liquid PFOA molecules. Therefore, we defined this temperature as the evaporation point (EP), characterized by an endothermic DSC peak at a temperature between the MP and the boiling point (BP).

Both MP and EP of PFCAs increased with the number of perfluorinated carbons (n_{CF2}), reaching ∼110 °C (MP) and 181−191 °C (EP) for PFUnDA (C11) (Figure 4a). A linear relationship between MP and EP and n_{CF2} was found:

$$\begin{aligned} &\text{MP } (^\circ\text{C}) = 19 \times n_{CF2} - 100\ (^\circ\text{C}) \\ &\quad ;\ (r = 0.99;\ p < 0.001;\ 95\%\text{CI} = 10 - 28 \\ &\quad \text{for the slope; four PFCAs in Figure 4a)} \end{aligned} \tag{8}$$

$$\begin{aligned} &\text{EP } (^\circ\text{C}) = 11 \times n_{CF2} + 69\ (^\circ\text{C}) \\ &\quad ;\ (r = 0.96;\ p < 0.001;\ 95\%\text{CI} = 8 - 14 \\ &\quad \text{for the slope; four PFCAs in Figure 4a)} \end{aligned} \tag{9}$$

An increase in one perfluorinated carbon unit (−CF_2−) led to a rise in the MP and EP of PFCAs by approximately 19 and 11 °C, respectively (eqs 8 and 9). The difference between MP and EP decreased with the chain length, ranging from 103 to 107 °C for PFOA (C8) to 72−81 °C for PFUnDA (C11) (Figures 4a and S25). In contrast, nonfluorinated counterparts (e.g., octanoic acid) have a much lower MP, a higher BP, and a wider temperature difference between MP and BP than PFCAs, resulting in lower volatility (Figure 5).

K-PFSAs had a higher MP (261−283 °C), a much higher EP (428−456 °C), and a wider difference (146−178 °C) between MP and EP than PFCAs, indicating that they are significantly less volatile than PFCAs (Figures 4a, 5, and S25). These findings are in agreement with the thermal degradation results (Figures 1 and 2). The solid-state phase predominated for K-PFSAs below 250 °C. The chain effect on the MP and EP of PFSA salts (i.e., K-PFASs) was not as significant as on those of PFCAs; an increase in one perfluorinated carbon unit (−CF_2−) in K-PFSAs led to a rise in MP by only 3 °C (eq 10) or no change in EP as shown in Figures 4a, 5, and S25:

$$\begin{aligned} &\text{MP } (^\circ\text{C}) = 3 \times n_{CF2} + 300\ (^\circ\text{C}) \\ &\quad ;\ (r = 0.64;\ p = 0.08;\ 95\%\text{CI} = -14 - 21 \\ &\quad \text{for the slope; three K} - \text{PFSAs in Figure 4a)} \end{aligned} \tag{10}$$

The DSC curves of K-PFBS and K-PFOS revealed a third endothermic peak (Figures S9, S14, and S16) in the high-temperature range (562−569 °C), coinciding with weight loss, suggesting thermal decomposition of the melt (liquid) K-PFBS and K-PFOS on the TGA sample crucible.

The MPs of the two cationic PFASs (PFOAAmS and PFOSAmS or C8-N-TAmP-FASA) were similar, ranging from 144 to 158 °C, which was higher than that of a zwitterionic PFAS (PFOAB, 95−105 °C) (Figure 4b). The EP values for these cationic and zwitterionic PFASs were 243−266 °C (Figure 4b).

The effect of the atmosphere (O_2 and N_2) on MPs and EPs was insignificant for the studied PFCAs, K-PFSAs, and cationic and zwitterionic polyfluorinated species (Figure 4). Previous research from our group indicated that the thermal degradation rate and extent of PFCAs and K-PFSAs were not significantly affected by the atmosphere (N_2, CO_2, O_2, and air).[29,30]

Using the weight loss data in TGA measurements (Figures S3 and S10), we determined the Arrhenius activation energy ($E_{A,evaporation}$) to be 105−113 kJ/mol corresponding to the evaporation of melted PFOA molecules at 116−149 °C. The value of $E_{A,evaporation}$ varied slightly between different atmospheres (O_2 and N_2) (Figure S26a and Table S3). Based on the thermal degradation data of gas-phase PFOA in a sealed reactor and in a nonpressured system (Figure S26b),[30,33] $E_{A,gas\text{-}phase\ degradation}$ was estimated at 77 kJ/mol in air or 87−89 kJ/mol in N_2 at 200−400 °C (eq 5; Table S3). A comparison of $E_{A,evaporation}$ and $E_{A,gas\text{-}phase\ degradation}$ suggests that the evaporation of melted PFOA molecules (eq 4) is a rate-limiting step, as illustrated in Figure 6.

For comparison, we also determined the values of $E_{A,evaporation}$ (287−360 kJ/mol) and $E_{A,gas\text{-}phase\ degradation}$ (121.4 kJ/mol) of K-PFOS (Figures 6 and S26 and Table S3). The result again suggests the evaporation of melted K-PFOS molecules as a rate-limiting step. The significant value of $E_{A,evaporation}$ for PFOS also indicates that PFOS is very nonvolatile relative to PFOA.

https://doi.org/10.1021/acsestengg.3c00114
ACS EST Engg. 2023, 3, 1370−1380

We observed that an increase in heating leads to slowed evaporation (Figure S27). An ultrafast heating rate can be achieved with induction heating during which the degradation of melted PFASs may occur (eqs 6 and 7 and Figure 6).

CONCLUSIONS

PFASs are a class of anthropogenic organic compounds widely used in industrial and commercial applications due to their unique chemical and physical properties. Despite the growing body of research on PFASs, there remain many knowledge gaps in the fundamental thermochemistry of these substances. Our work has provided unequivocal evidence that PFAS molecules undergo melting and then an evaporating stage during thermal decomposition. This is the first study, to the best of our knowledge, that compares the thermal phase transition and thermal degradation processes of PFASs. MPs and EPs of many PFASs were reported for the first time. Our thermogravimetric data also support the thermal decomposition of melted PFASs. The thermogravimetric data, together with the degradation results, support the phase transitions (e.g., evaporation) of PFOA and PFOS as a rate-limiting step. This finding may be applicable to other nonvolatile PFAS compounds at room temperature, which calls for further investigation.

Another contribution of this study is the development of a fast-degradation method for PFASs in spent media. PFASs generally resist degradation, posing considerable challenges to established water treatment and waste disposal practices. The removal and degradation of PFASs from water can be achieved by various approaches, such as photocatalytic degradation,[63−66] reductive defluorination,[67−69] enhanced adsorption,[70−73] electrochemical approaches,[74−77] supercritical water oxidation,[78−80] plasma[81,82] and nonthermal plasma,[83,84] and hydrothermal methods assisted with base[85−87] and aprotic solvents.[43] However, much fewer options are available to handle solid materials containing PFASs.[88,89] In this study, we have demonstrated that the innovative approach of induction heating can significantly degrade PFASs in spent media within a short period. Unlike conventional slow heating methods, induction heating rapidly increases the temperature, enabling it to pass quickly through the low and moderate temperature range where many fluorinated PFAS species are likely to be generated.[31−33] Furthermore, induction heating requires minimal time to reach a desired temperature and cool down, making it highly energy-efficient and much faster than conventional thermal methods. This PFAS thermal degradation approach does not need to be performed in a continuous operation and is potentially "low-tech" and inexpensive for reactivation of spent media (Figures 1 and 2). It is effective for PFSAs (e.g., PFOS) and short-chain PFASs (Figures 1 and 2). Additionally, the induction heating process is also inherently safer than other heating methods as it does not involve combustion or open flame.

Lastly, while induction heating offers many advantages, it has some drawbacks. One major drawback is the corrosion of the metallic reactor. We have separately studied the yield of F from PFASs upon heating.[29,33] The mineralization rate of PFOA and PFOS can reach 92 mol % with increasing temperature to ≥700 °C.[29] In the present study, the internal corrosion of the reactor was seen after use, suggesting that reactive F species (e.g., F· and HF) react with the steel reactor species producing insoluble metal fluoride.[90−92] This is substantiated by the ∼90% reduction of measurable F when PFOA was heated in the steel reactor (see SI). Our recent study has demonstrated that kaolinite can dramatically decrease the emission of F from PFASs upon heating.[30] Therefore, adding kaolinite to the reactor may mitigate the corrosion of the reaction, which warrants further studies.

ASSOCIATED CONTENT

Supporting Information

The Supporting Information is available free of charge at https://pubs.acs.org/doi/10.1021/acsestengg.3c00114.

Thermal decomposition of PFOA and PFOS in a tube furnace, additional experimental procedures, analysis of PFASs and the UPLC−QToF-MS/MS method; measurement of the yield of F, determination of extraction efficiency, PFASs used in this study; temperatures of the reactor monitored by two approaches; Arrhenius activation energies for PFOA and K-PFOS in thermal phase transition and decomposition processes in different atmospheres; experimental setup, pore size distribution of Filtrasorb 200; TGA, DTG, and DSC curves of PFCAs, K-PFSAs, and polyfluoroalkyl substances; correlations between the MPs/EPs of PFCAs and K-PFSAs and the number of perfluorinated carbons; Arrhenius plots for PFOA and K-PFOS based on isothermal TGA scan data and thermal decomposition data in a sealed reactor; TGA of PFOA at different heating rates in an atmosphere of N_2 (PDF)

AUTHOR INFORMATION

Corresponding Author

Feng Xiao − *Department of Civil and Environmental Engineering, University of Missouri, Columbia, Missouri 65211, United States;* orcid.org/0000-0001-5686-6055; Phone: +1-573-882-0107; Email: feng.xiao@missouri.edu, fxiaoee@gmail.com

Authors

Pavankumar Challa Sasi − *Department of Civil Engineering, University of North Dakota, Grand Forks, North Dakota 58202, United States; EA Engineering, Science, and Technology, Inc., Hunt Valley, Maryland 21031, United States*

Ali Alinezhad − *Department of Civil and Environmental Engineering, University of Missouri, Columbia, Missouri 65211, United States*

Runze Sun − *Department of Civil and Environmental Engineering, University of Missouri, Columbia, Missouri 65211, United States*

Mansurat Abdulmalik Ali − *Department of Civil Engineering, University of North Dakota, Grand Forks, North Dakota 58202, United States*

Complete contact information is available at: https://pubs.acs.org/10.1021/acsestengg.3c00114

Author Contributions

F.X. contributed to the overall conception on induction heating of PFASs and design of the study and the manuscript preparation. P.C.S., A.A., and R.S. contributed to experimental execution. M.A.A. contributed to TGA and DSC analyses of PFASs. All authors contributed to experimental design and data analysis and plotting. CRediT: **Feng Xiao** conceptualization, data curation, formal analysis, funding acquisition,

https://doi.org/10.1021/acsestengg.3c00114
ACS EST Engg. 2023, 3, 1370−1380

investigation, methodology, project administration, resources, supervision, writing-original draft, writing-review & editing; **Pavankumar Challa Sasi** data curation, formal analysis, software; **Ali Alinezhad** data curation, formal analysis, validation; **Runze Sun** formal analysis, software; **Mansurat Abdulmalik Ali** formal analysis, validation.

Notes

The authors declare no competing financial interest.

■ ACKNOWLEDGMENTS

This work was partially supported by the U.S. National Science Foundation CAREER Program (2047062) and the DoD SERDP Program (ER22-4014). P.C.S. and A.A. were also supported by graduate fellowships supported by the U.S. Geological Survey (FAR0032661 and FAR35039). F.X. also thanks Dr. Mikhail Golovko for allowing to use UPLC−QToF-MS/MS, available in the Department of Biomedical Sciences at the University of North Dakota. Any opinions, findings, and conclusions or recommendations expressed in this material are those of the author(s) and do not necessarily reflect the views of the NSF and DoD.

■ REFERENCES

(1) Whitehead, H. D.; Venier, M.; Wu, Y.; Eastman, E.; Urbanik, S.; Diamond, M. L.; Shalin, A.; Schwartz-Narbonne, H.; Bruton, T. A.; Blum, A.; Wang, Z. Y.; Green, M.; Tighe, M.; Wilkinson, J. T.; McGuinness, S.; Peaslee, G. F. Fluorinated compounds in North American cosmetics. *Environ. Sci. Tech. Lett.* **2021**, *8*, 538−544.

(2) Muensterman, D. J.; Cahuas, L.; Titaley, I. A.; Schmokel, C.; De la Cruz, F. B.; Barlaz, M. A.; Carignan, C. C.; Peaslee, G. F.; Field, J. A. Per- and polyfluoroalkyl substances (PFAS) in facemasks: Potential source of human exposure to PFAS with implications for disposal to landfills. *Environ. Sci. Tech. Lett.* **2022**, *9*, 320−326.

(3) Schaider, L. A.; Balan, S. A.; Blum, A.; Andrews, D. Q.; Strynar, M. J.; Dickinson, M. E.; Lunderberg, D. M.; Lang, J. R.; Peaslee, G. F. Fluorinated compounds in U.S. fast food packaging. *Environ. Sci. Technol. Lett.* **2017**, *4*, 105−111.

(4) Glenn, G.; Shogren, R.; Jin, X.; Orts, W.; Hart-Cooper, W.; Olson, L. Per- and polyfluoroalkyl substances and their alternatives in paper food packaging. *Compr. Rev. Food Sci. Food Saf.* **2021**, *20*, 2596−2625.

(5) Sajid, M.; Ilyas, M. PTFE-coated non-stick cookware and toxicity concerns: A perspective. *Environ. Sci. Pollut. Res.* **2017**, *24*, 23436−23440.

(6) Kotthoff, M.; Muller, J.; Jurling, H.; Schlummer, M.; Fiedler, D. Perfluoroalkyl and polyfluoroalkyl substances in consumer products. *Environ. Sci. Pollut. Res. Int.* **2015**, *22*, 14546−14559.

(7) Barzen-Hanson, K. A.; Roberts, S. C.; Choyke, S.; Oetjen, K.; McAlees, A.; Riddell, N.; McCrindle, R.; Ferguson, P. L.; Higgins, C. P.; Field, J. A. Discovery of 40 classes of per- and polyfluoroalkyl substances in historical aqueous film-forming foams (AFFFs) and AFFF-impacted groundwater. *Environ. Sci. Technol.* **2017**, *51*, 2047−2057.

(8) D'Agostino, L. A.; Mabury, S. A. Identification of novel fluorinated surfactants in aqueous film forming foams and commercial surfactant concentrates. *Environ. Sci. Technol.* **2014**, *48*, 121−129.

(9) Giesy, J. P.; Kannan, K. Global distribution of perfluorooctane sulfonate in wildlife. *Environ. Sci. Technol.* **2001**, *35*, 1339−1342.

(10) Houde, M.; De Silva, A. O.; Muir, D. C.; Letcher, R. J. Monitoring of perfluorinated compounds in aquatic biota: An updated review. *Environ. Sci. Technol.* **2011**, *45*, 7962−7973.

(11) Xiao, F. Emerging poly- and perfluoroalkyl substances in the aquatic environment: A review of current literature. *Water Res.* **2017**, *124*, 482−495.

(12) Houtz, E. F.; Higgins, C. P.; Field, J. A.; Sedlak, D. L. Persistence of perfluoroalkyl acid precursors in AFFF-impacted groundwater and soil. *Environ. Sci. Technol.* **2013**, *47*, 8187−8195.

(13) Evich, M. G.; Davis, M. J. B.; McCord, J. P.; Acrey, B.; Awkerman, J. A.; Knappe, D. R. U.; Lindstrom, A. B.; Speth, T. F.; Tebes-Stevens, C.; Strynar, M. J.; Wang, Z. Y.; Weber, E. J.; Henderson, W. M.; Washington, J. W. Per- and polyfluoroalkyl substances in the environment. *Science* **2022**, *375*, No. eabg9065.

(14) USEPA. PFAS Strategic Roadmap: EPA's Commitments to Action 2021−2024. https://www.epa.gov/system/files/documents/2021-10/pfas-roadmap_final-508.pdf (accessed March 2022). 2021.

(15) USEPA. Announcement of final regulatory determinations for contaminants on the fourth drinking water contaminant candidate list. *Fed. Regist.* **2021**, *86*, 12272−12291.

(16) EU. Directive (EU) 2020/2184 of the European Parliament and of the Council of 16 December 2020 on the quality of water intended for human consumption. https://eur-lex.europa.eu/eli/dir/2020/2184/oj (accessed July 2022). 2020.

(17) HealthCanada. Guidelines for Canadian Drinking Water Quality: Guideline Technical Document − Perfluorooctanoic Acid (PFOA) https://www.canada.ca/en/health-canada/services/publications/healthy-living/guidelines-canadian-drinking-water-quality-technical-document-perfluorooctanoic-acid/document.html#s12 (accessed June 2019). 2018.

(18) HealthCanada. Guidelines for Canadian Drinking Water Quality: Guideline Technical Document − Perfluorooctane Sulfonate (PFOS). https://www.canada.ca/en/health-canada/services/publications/healthy-living/guidelines-canadian-drinking-water-quality-guideline-technical-document-perfluorooctane-sulfonate/document.html (accessed June 2019). 2018.

(19) MOH. Ministry of Health of the PR China. Standard for Drinking Water Quality (GB 5749-2022). https://www.chinesestandard.net/PDF/English.aspx/GB5749-2022 (accessed August 2022). 2022.

(20) Rahman, M. F.; Peldszus, S.; Anderson, W. B. Behaviour and fate of perfluoroalkyl and polyfluoroalkyl substances (PFASs) in drinking water treatment: A review. *Water Res.* **2014**, *50*, 318−340.

(21) Herkert, N. J.; Merrill, J.; Peters, C.; Bollinger, D.; Zhang, S.; Hoffman, K.; Ferguson, P. L.; Knappe, D. R. U.; Stapleton, H. M. Assessing the Effectiveness of Point-of-Use Residential Drinking Water Filters for Perfluoroalkyl Substances (PFASs). *Environ. Sci. Technol. Lett.* **2020**, *7*, 178−184.

(22) Chow, S. J.; Croll, H. C.; Ojeda, N.; Klamerus, J.; Capelle, R.; Oppenheimer, J.; Jacangelo, J. G.; Schwab, K. J.; Prasse, C. Comparative investigation of PFAS adsorption onto activated carbon and anion exchange resins during long-term operation of a pilot treatment plant. *Water Res.* **2022**, *226*, No. 119198.

(23) Chen, R.; Huang, X.; Li, G.; Yu, Y.; Shi, B. Performance of in-service granular activated carbon for perfluoroalkyl substances removal under changing water quality conditions. *Sci. Total Environ.* **2022**, *848*, No. 157723.

(24) Burkhardt, J. B.; Burns, N.; Mobley, D.; Pressman, J. G.; Magnuson, M. L.; Speth, T. F. Modeling PFAS Removal Using Granular Activated Carbon for Full-Scale System Design. *J. Environ. Eng.* **2022**, *148*, No. 04021086.

(25) Fang, Y.; Ellis, A.; Choi, Y. J.; Boyer, T. H.; Higgins, C. P.; Schaefer, C. E.; Strathmann, T. J. Removal of Per- and Polyfluoroalkyl Substances (PFASs) in Aqueous Film-Forming Foam (AFFF) Using Ion-Exchange and Nonionic Resins. *Environ. Sci. Technol.* **2021**, *55*, 5001−5011.

(26) Ellis, A. E.; Liu, C. J.; Fang, Y.; Boyer, T. H.; Schaefer, C. E.; Higgins, C. P.; Strathmann, T. J. Pilot study comparison of regenerable and emerging single-use anion exchange resins for treatment of groundwater contaminated by per- and polyfluoroalkyl substances (PFASs). *Water Res.* **2022**, *223*, No. 119019.

(27) Liu, Y. L.; Sun, M. Ion exchange removal and resin regeneration to treat per- and polyfluoroalkyl ether acids and other emerging PFAS in drinking water. *Water Res.* **2021**, *207*, No. 117781.

https://doi.org/10.1021/acsestengg.3c00114
ACS EST Engg. 2023, 3, 1370−1380

(28) Boyer, T. H.; Ellis, A.; Fang, Y. D.; Schaefer, C. E.; Higgins, C. P.; Strathmann, T. J. Life cycle environmental impacts of regeneration options for anion exchange resin remediation of PFAS impacted water. *Water Res.* **2021**, *207*, No. 117798.
(29) Xiao, F.; Sasi, P. C.; Yao, B.; Kubatova, A.; Golovko, S. A.; Golovko, M. Y.; Soli, D. Thermal stability and decomposition of perfluoroalkyl substances on spent granular activated carbon. *Environ. Sci. Tech. Lett.* **2020**, *7*, 343−350.
(30) Alinezhad, A.; Sasi, P. C.; Yao, B.; Kubatova, A.; Golovko, S. A.; Golovko, M. Y.; Xiao, F. An investigation of thermal air degradation and pyrolysis of per- and polyfluoroalkyl substances and aqueous film-forming foams in soil. *ACS EST Eng.* **2022**, *2*, 198−209.
(31) Xiao, F.; Sasi, P. C.; Alinezhad, A.; Golovko, S. A.; Golovko, M. Y.; Spoto, A. Thermal decomposition of anionic, awitterionic, and cationic polyfluoroalkyl substances in aqueous film-forming foams. *Environ. Sci. Technol.* **2021**, *55*, 9885−9894.
(32) Yao, B.; Sun, R.; Alinezhad, A.; Kubatova, A.; Simcik, M. F.; Guan, X.; Xiao, F. The first quantitative investigation of compounds generated from PFAS, PFAS-containing aqueous film-forming foams and commercial fluorosurfactants in pyrolytic processes. *J. Hazard. Mater.* **2022**, *436*, No. 129313.
(33) Sasi, P. C.; Alinezhad, A.; Yao, B.; Kubatova, A.; Golovko, S. A.; Golovko, M. Y.; Xiao, F. Effect of granular activated carbon and other porous materials on thermal decomposition of per- and polyfluoroalkyl substances: Mechanisms and implications for water purification. *Water Res.* **2021**, *200*, No. 117271.
(34) Longendyke, G. K.; Katel, S.; Wang, Y. X. PFAS fate and destruction mechanisms during thermal treatment: A comprehensive review. *Environ. Sci. Process. Impacts* **2022**, *24*, 196−208.
(35) Wang, J.; Lin, Z.; He, X.; Song, M.; Westerhoff, P.; Doudrick, K.; Hanigan, D. Critical review of thermal decomposition of per- and polyfluoroalkyl substances: Mechanisms and implications for thermal treatment processes. *Environ. Sci. Technol.* **2022**, *56*, 5355−5370.
(36) Xiao, F.; Sasi, P. C.; Yao, B.; Kubatova, A.; Golovko, S. A.; Golovko, M. Y.; Soli, D. Thermal Decomposition of PFAS: Response to Comment on "Thermal Stability and Decomposition of Perfluoroalkyl Substances on Spent Granular Activated Carbon". *Environ. Sci. Tech. Lett.* **2021**, *8*, 364−365.
(37) Watanabe, N.; Takata, M.; Takemine, S.; Yamamoto, K. Thermal mineralization behavior of PFOA, PFHxA, and PFOS during reactivation of granular activated carbon (GAC) in nitrogen atmosphere. *Environ. Sci. Pollut. Res. Int.* **2018**, *25*, 7200−7205.
(38) Duchesne, A. L.; Brown, J. K.; Patch, D. J.; Major, D.; Weber, K. P.; Gerhard, J. I. Remediation of PFAS-contaminated soil and granular activated carbon by smoldering combustion. *Environ. Sci. Technol.* **2020**, *54*, 12631.
(39) DiStefano, R.; Feliciano, T.; Mimna, R. A.; Redding, A. M.; Matthis, J. Thermal destruction of PFAS during full-scale reactivation of PFAS-laden granular activated carbon. *Remediation* **2022**, *32*, 231−238.
(40) Dastgheib, S. A.; Mock, J.; Ilangovan, T.; Patterson, C. Thermogravimetric studies for the incineration of an anion exchange resin laden with short- or long-chain PFAS compounds containing carboxylic or sulfonic acid functionalities in the presence or absence of calcium oxide. *Ind. Eng. Chem. Res.* **2021**, *60*, 16961−16968.
(41) Thoma, E. D.; Wright, R. S.; George, I.; Krause, M.; Presezzi, D.; Villa, V.; Preston, W.; Deshmukh, P.; Kauppi, P.; Zemek, P. G. Pyrolysis processing of PFAS-impacted biosolids, a pilot study. *J. Air Waste Manag. Assoc.* **2022**, *72*, 309−318.
(42) Zhang, W. L.; Cao, H. M.; Mahadevan, S.; Savage, P.; Liang, Y. N. Destruction of perfluoroalkyl acids accumulated in *Typha latifolia* through hydrothermal liquefaction. *ACS Sustainable Chem. Eng.* **2020**, *8*, 9257−9262.
(43) Trang, B.; Li, Y.; Xue, X. S.; Ateia, M.; Houk, K. N.; Dichtel, W. R. Low-temperature mineralization of perfluorocarboxylic acids. *Science* **2022**, *377*, 839−845.
(44) Crownover, E.; Oberle, D.; Kluger, M.; Heron, G. Perfluoroalkyl and polyfluoroalkyl substances thermal desorption evaluation. *Remediation* **2019**, *29*, 77−81.
(45) Hutzinger, O.; Choudhry, G. G.; Chittim, B. G.; Johnston, L. E. Formation of polychlorinated dibenzofurans and dioxins during combustion, electrical equipment fires and PCB incineration. *Environ. Health Perspect.* **1985**, *60*, 3−9.
(46) Dyke, P. H.; Foan, C.; Fiedler, H. PCB and PAH releases from power stations and waste incineration processes in the UK. *Chemosphere* **2003**, *50*, 469−480.
(47) Dopico, M.; Gomez, A. Review of the current state and main sources of dioxins around the world. *J. Air Waste Manag. Assoc.* **2015**, *65*, 1033−1049.
(48) Soderstrom, G.; Marklund, S. PBCDD and PBCDF from incineration of waste-containing brominated flame retardants. *Environ. Sci. Technol.* **2002**, *36*, 1959−1964.
(49) DoD. Temporary Prohibition on Incineration of Materials Containing Per- and Polyfluoroalkyl Substances (PFAS). https://media.defense.gov/2022/Apr/28/2002986273/-1/-1/1/TEMPORARY-PROHIBITION-ON-INC%5B%E2%80%A6%5DNG-PRE-AND-POLYFLUOROALKYL-SUBSTANCES-PFAS-APRIL-26-2022.PDF (accessed December 2022). 2022.
(50) Zinn, S.; Semiatin, S. L. *Elements of Induction Heating: Design Control and Applications*; Electric Power Research Institute, Inc.: 1988.
(51) Jin, B.; Mallula, S.; Golovko, S. A.; Golovko, M. Y.; Xiao, F. In vivo generation of PFOA, PFOS, and other compounds from cationic and zwitterionic per- and polyfluoroalkyl substances in a terrestrial invertebrate (Lumbricus terrestris). *Environ. Sci. Technol.* **2020**, *54*, 7378−7387.
(52) Xiao, F.; Jin, B.; Golovko, S. A.; Golovko, M. Y.; Xing, B. Sorption and desorption mechanisms of cationic and zwitterionic per- and polyfluoroalkyl substances in natural soils: Thermodynamics and hysteresis. *Environ. Sci. Technol.* **2019**, *53*, 11818−11827.
(53) Tsuji, M.; Inoue, T.; Shibata, O. Purification and thermal analysis of perfluoro-n-alkanoic acids. *Colloids Surf., B* **2008**, *61*, 61−65.
(54) Gabbott, P. *Principles and Applications of Thermal Analysis*; John Wiley & Sons: Oxford, UK, 2008.
(55) Yao, F.; Wu, Q. L.; Lei, Y.; Guo, W. H.; Xu, Y. J. Thermal decomposition kinetics of natural fibers: Activation energy with dynamic thermogravimetric analysis. *Polym. Degrad. Stab.* **2008**, *93*, 90−98.
(56) Baghirzade, B. S.; Zhang, Y.; Reuther, J. F.; Saleh, N. B.; Venkatesan, A. K.; Apul, O. G. Thermal regeneration of spent granular activated carbon presents an opportunity to break the forever PFAS cycle. *Environ. Sci. Technol.* **2021**, *55*, 5608−5619.
(57) Jin, Z. Q.; Tian, B.; Wang, L. W.; Wang, R. Z. Comparison on Thermal Conductivity and Permeability of Granular and Consolidated Activated Carbon for Refrigeration. *Chinese J. Chem. Eng.* **2013**, *21*, 676−682.
(58) Khaliji Oskouei, M.; Tamainot-Telto, Z. Investigation of the heat transfer properties of granular activated carbon with R723 for adsorption refrigeration and heat pump. *Therm. Sci. Eng. Prog.* **2019**, *12*, 1.
(59) Engineering ToolBox. Air - Thermal Conductivity. [online] https://www.engineeringtoolbox.com/air-properties-viscosity-conductivity-heat-capacity-d_1509.html (accessed May 2020). 2009
(60) Zhang, M.; Yamada, K.; Bourguet, S.; Guelfo, J.; Suuberg, E. M. Vapor pressure of nine perfluoroalkyl substances (PFASs) determined using the Knudsen Effusion Method. *J. Chem. Eng. Data* **2020**, *65*, 2332−2342.
(61) PubChem. Melting point of perfluorooctanoic acid. https://pubchem.ncbi.nlm.nih.gov/compound/Perfluorooctanoic-acid#section=Boiling-Point (accessed September 2021).
(62) SciFinder CAS. Melting point of K-PFOS. https://scifinder-n.cas.org/searchDetail/substance/61b9152c10d6ab46281d280b/substanceDetails (accessed September 2021).
(63) Bentel, M. J.; Liu, Z. K.; Yu, Y. C.; Gao, J. Y.; Men, Y. J.; Liu, J. Y. Enhanced degradation of perfluorocarboxylic acids (PFCAs) by UV/sulfite treatment: Reaction mechanisms and system efficiencies at pH 12. *Environ. Sci. Tech. Lett.* **2020**, *7*, 351−357.

https://doi.org/10.1021/acsestengg.3c00114
ACS EST Engg. 2023, 3, 1370−1380

(64) Qanbarzadeh, M.; Wang, D. W.; Ateia, M.; Sahu, S. P.; Cates, E. L. Impacts of reactor configuration, degradation mechanisms, and water matrices on perfluorocarboxylic acid treatment efficiency by the UV/$Bi_3O(OH)(PO_4)_2$ photocatalytic process. *ACS EST Eng.* **2021**, *1*, 239−248.
(65) Tenorio, R.; Liu, J. Y.; Xiao, X.; Maizel, A.; Higgins, C. P.; Schaefer, C. E.; Strathmann, T. J. Destruction of per- and polyfluoroalkyl substances (PFASs) in aqueous film-forming foam (AFFF) with UV-sulfite photoreductive treatment. *Environ. Sci. Technol.* **2020**, *54*, 6957−6967.
(66) Liu, F. Q.; Guan, X. H.; Xiao, F. Photodegradation of per- and polyfluoroalkyl substances in water: A review of fundamentals and applications. *J. Hazard. Mater.* **2022**, *439*, No. 129580.
(67) Cheng, Z. W.; Chen, Q. C.; Liu, Z. K.; Liu, J. Y.; Liu, Y. W.; Liu, S. Q.; Gao, X. P.; Tan, Y. J.; Shen, Z. M. Interpretation of reductive PFAS defluorination with quantum chemical parameters. *Environ. Sci. Tech. Lett.* **2021**, *8*, 645−650.
(68) Cui, J. K.; Gao, P. P.; Deng, Y. Destruction of Per- and Polyfluoroalkyl Substances (PFAS) with Advanced Reduction Processes (ARPs): A Critical Review. *Environ. Sci. Technol.* **2020**, *54*, 3752−3766.
(69) Biswas, S.; Yamijala, S. S. R. K. C.; Wong, B. M. Degradation of Per- and Polyfluoroalkyl Substances with Hydrated Electrons: A New Mechanism from First-Principles Calculations. *Environ. Sci. Technol.* **2022**, *56*, 8167−8175.
(70) Verduzco, R.; Wong, M. S. Fighting PFAS with PFAS. *ACS Central Sci.* **2020**, *6*, 453−455.
(71) Kumarasamy, E.; Manning, I.; Collins, L. B.; Coronell, O.; Leibfarth, F. Ionic fluorogels for remediation of per- and polyfluorinated alkyl substances from water. *ACS Central Sci.* **2020**, *6*, 487−492.
(72) Dixit, F.; Munoz, G.; Mirzaei, M.; Barbeau, B.; Liu, J.; Duy, S. V.; Sauve, S.; Kandasubramanian, B.; Mohseni, M. Removal of zwitterionic PFAS by MXenes: Comparisons with anionic, nonionic, and PFAS-specific resins. *Environ. Sci. Technol.* **2022**, *56*, 6212−6222.
(73) Garg, S.; Wang, J. S.; Kumar, P.; Mishra, V.; Arafat, H.; Sharma, R. S.; Dumee, L. F. Remediation of water from per−/poly-fluoroalkyl substances (PFAS) - Challenges and perspectives. *J. Environ. Chem. Eng.* **2021**, *9*, No. 105784.
(74) Schaefer, C. E.; Choyke, S.; Ferguson, P. L.; Andaya, C.; Burant, A.; Maizel, A.; Strathmann, T. J.; Higgins, C. P. Electrochemical transformations of perfluoroalkyl acid (PFAA) precursors and PFAAs in groundwater impacted with aqueous film forming foams. *Environ. Sci. Technol.* **2018**, *52*, 10689−10697.
(75) Le, T. X. H.; Haflich, H.; Shah, A. D.; Chaplin, B. P. Energy-efficient electrochemical oxidation of perfluoroalkyl substances using a Ti4O7 reactive electrochemical membrane anode. *Environ. Sci. Tech. Lett.* **2019**, *6*, 504−510.
(76) Sharma, S.; Shetti, N. P.; Basu, S.; Nadagouda, M. N.; Aminabhavi, T. M. Remediation of per- and polyfluoroalkyls (PFAS) via electrochemical methods. *Chem. Eng. J.* **2022**, *430*, No. 132895.
(77) Shanbhag, M. M.; Shetti, N. P.; Kalanur, S. S.; Pollet, B. G.; Nadagouda, M. N.; Aminabhavi, T. M. Hafnium doped tungsten oxide intercalated carbon matrix for electrochemical detection of perfluorooctanoic acid. *Chem. Eng. J.* **2022**, *434*, No. 134700.
(78) Li, J. N.; Austin, C.; Moore, S.; Pinkard, B. R.; Novosselov, I. V. PFOS destruction in a continuous supercritical water oxidation reactor. *Chem. Eng. J.* **2023**, *451*, No. 139063.
(79) Krause, M. J.; Thoma, E.; Sahle-Damesessie, E.; Crone, B.; Whitehill, A.; Shields, E.; Gullett, B. Supercritical Water Oxidation as an Innovative Technology for PFAS Destruction. *J. Environ. Eng.* **2022**, *148*, No. 05021006.
(80) McDonough, J. T.; Kirby, J.; Bellona, C.; Quinnan, J. A.; Welty, N.; Follin, J.; Liberty, K. Validation of supercritical water oxidation to destroy perfluoroalkyl acids. *Remediation* **2022**, *32*, 75−90.
(81) Singh, R. K.; Multari, N.; Nau-Hix, C.; Woodard, S.; Nickelsen, M.; Thagard, S. M.; Holsen, T. M. Removal of Poly- and Per-Fluorinated Compounds from Ion Exchange Regenerant Still Bottom Samples in a Plasma Reactor. *Environ. Sci. Technol.* **2020**, *54*, 13973−13980.
(82) Singh, R. K.; Multari, N.; Nau-Hix, C.; Anderson, R. H.; Richardson, S. D.; Holsen, T. M.; Thagard, S. M. Rapid Removal of Poly- and Perfluorinated Compounds from Investigation-Derived Waste (IDW) in a Pilot-Scale Plasma Reactor. *Environ. Sci. Technol.* **2019**, *53*, 11375−11382.
(83) Lewis, A. J.; Joyce, T.; Hadaya, M.; Ebrahimi, F.; Dragiev, I.; Giardetti, N.; Yang, J. C.; Fridman, G.; Rabinovich, A.; Fridman, A. A.; Mckenzie, E. R.; Sales, C. M. Rapid degradation of PFAS in aqueous solutions by reverse vortex flow gliding arc plasma. *Environ. Sci. Water Res. Technol.* **2020**, *6*, 1044−1057.
(84) Rabinovich, A.; Nirenberg, G.; Kocagoz, S.; Surace, M.; Sales, C.; Fridman, A. Scaling Up of Non-Thermal Gliding Arc Plasma Systems for Industrial Applications. *Plasma Chem. Plasma Process.* **2022**, *42*, 35−50.
(85) Wu, B. R.; Hao, S. L.; Choi, Y. J.; Higgins, C. P.; Deeb, R.; Strathmann, T. J. Rapid destruction and defluorination of perfluorooctanesulfonate by alkaline hydrothermal reaction. *Environ. Sci. Tech. Lett.* **2019**, *6*, 630−636.
(86) Hao, S.; Choi, Y. J.; Wu, B.; Higgins, C. P.; Deeb, R.; Strathmann, T. J. Hydrothermal alkaline treatment for destruction of per- and polyfluoroalkyl substances in aqueous film-forming foam. *Environ. Sci. Technol.* **2021**, *55*, 3283−3295.
(87) Zhang, W. L.; Liang, Y. N. Effects of hydrothermal treatments on destruction of per- and polyfluoroalkyl substances in sewage sludge. *Environ. Pollut.* **2021**, *285*, No. 117276.
(88) Winchell, L. J.; Ross, J. J.; Wells, M. J. M.; Fonoll, X.; Norton, J. W.; Bell, K. Y. Per- and polyfluoroalkyl substances thermal destruction at water resource recovery facilities: A state of the science review. *Water Environ. Res.* **2021**, *93*, 826−843.
(89) Munoz, G.; Michaud, A. M.; Liu, M.; Duy, S. V.; Montenach, D.; Resseguier, C.; Watteau, F.; Sappin-Didier, V.; Feder, F.; Morvan, T.; Houot, S.; Desrosiers, M.; Liu, J. X.; Sauve, S. Target and Nontarget Screening of PFAS in Biosolids, Composts,and Other Organic Waste Products for Land Application in France. *Environ. Sci. Technol.* **2022**, *56*, 6056−6068.
(90) Zou, G. B.; Shi, W.; Xiang, S.; Ji, X. M.; Ma, G. Q.; Ballinger, R. G. Corrosion behavior of 904L austenitic stainless steel in hydrofluoric acid. *RSC Adv.* **2018**, *8*, 2811−2817.
(91) Capps, N. E.; Mackie, N. M.; Fisher, E. R. Surface interactions of CF2 radicals during deposition of amorphous fluorocarbon films from CHF3 plasmas. *J. Appl. Phys.* **1998**, *84*, 4736−4743.
(92) Dai, H. L.; Shi, S. W.; Yang, L.; Guo, C.; Chen, X. Recent progress on the corrosion behavior of metallic materials in HF solution. *Corros. Rev.* **2021**, *39*, 313−337.

https://doi.org/10.1021/acsestengg.3c00114
ACS EST Engg. 2023, 3, 1370−1380